sciendo

POLISH MARITIME RESEARCH Special Issue 2018 S3 (99) 2018 Vol. 25; pp. 120-126
10.2478/pomr-2018-0120

EFFECT OF REINFORCEMENT RATIO AND VERTICAL LOAD LEVEL ON LATERAL CAPACITY OF BRIDGE PILE FOUNDATIONS

Fan Qinglai [1)]
Gao Yufeng [2)]
[1)] School of Civil Engineering, Ludong University, China
[2)] College of Civil and Transportation Engineering, Hohai University, China

ABSTRACT

The bearing response of pile foundations for cross-sea bridge subjected to lateral loading is investigated through three-dimensional finite element numerical analyses. In the analyses, non-linear behavior of concrete is simulated using smeared cracking model, and the strain-stress relationship of rebar is modeled through perfectly elasto-plastic model obeying Mises yield criterion. The finite element model is validated against published lateral static loading test in situ. The effect of reinforcement ratio of reinforced concrete and vertical load level is explored on the displacement of pile head and lateral capacity of pile. The results show that for the pile with low reinforcement ratio, the allowable lateral capacity is controlled by concrete cracking, however the allowable lateral capacity is controlled by the displacement of pile head with high reinforcement ratio. The vertical load applied on the pile head may reduce its displacement but increase simultaneously the maximum moment in the pile body. Therefore, the optimum vertical load level is 0.4~0.6 times of the vertical ultimate load of a single pile.

Keywords: cross-sea bridge, pile foundations, lateral capacity, concrete damage, numerical analysis

INTRODUCTION

In the last few decades, the bored pile foundation has been widely utilized in cross-sea bridges. In the marine environment, the pile foundation not only bears the vertical load caused by self weight of upper structure and pile body, but also bears lateral load induced by wave, wind and vehicle braking, etc. Under the extreme sea conditions, pile foundations are always subjected to large horizontal load, therefore two kinds of failure modes may occur, including plastic failure of soil around pile and concrete damage and rebar yielding of pile body. Most of the available numerical analyses have assumed that the pile is linear elastic [1-6]. In fact, in these studies, only the influence of plastic flow of soil around the pile on the lateral capacity is actually analyzed, but the effect of concrete damage and rebar yielding of pile body is not considered. Using finite element method, Zheng and Wang [7] analyzed the effect of level as well as sequence of vertical and lateral load on the capacity of single pile. The concrete and rebar were simulated through plastic damage model and linear elastic model respectively in their finite element method. The computation results showed that the long pile and short pile exhibit different deformation characteristic. Through similar method, the influence of reinforcement ratio, pile head constraint and vertical load level was investigated on response of small diameter cast-in-place pile by Cai et al [8]. Through comparison of results of in-situ test and numerical analysis, Conte et al. [9] concluded that under large horizontal load, the displacement of pile head may be underestimated considerably without considering the damage of concrete and

reinforcement yielding. However, the determination method of ultimate capacity of single pile is not proposed in their work. Therefore, the lateral bearing response of single pile is studied considering concrete damage and rebar yield in the paper. The effect of reinforcement ratio of reinforced concrete and vertical load level is explored on the displacement of pile head and lateral capacity of pile. The determination method of ultimate lateral capacity is proposed.

FINITE ELEMENT MODEL

The in-situ horizontal load test for large diameter reinforced concrete pile was carried out by Huang etc [10]. In this present study, the results from the horizontal loading test conducted on a single pile with diameter D=1.5m and embedment depth L=34m are considered. The reinforcement consisted of 52ϕ32 bars arranged in two rings. The properties of the concrete and rebar are showed in Table 1. A hydraulic jack was utilized to apply the lateral load at the pile head which is off the ground surface by about 0.9m. The stratification of the subsoil and the corresponding parameters are indicated in Table 2. In particular, the dilatancy angle ψ, is evaluated using the following empirical relationship [11]: for the soil layer with internal friction angle ψ less than 30°, a value of $\psi = 0$ is assumed, however for the layer with $\varphi > 30°$, the value of dilatancy angle is calculated using the expression with $\psi = \varphi - 30°$.

In order to indentify the applicability of finite element method, the in situ test is simulated numerically in this paper. A linear elastic perfectly plastic model with Mohr-Coulomb failure criterion is used for modelling the soil behaviour. The stress-strain relationship of steel rebar is elastic perfectly plastic with Mises failure criterion. The reinforcement is assumed to be smeared in concrete and is fully bonded to it. The concrete is modelled with smeared cracking model proposed by Hillerborg etc [12, 13]. In the model, it is assumed that the concrete material follows the plasticity theory under compression condition, and obeys fracture mechanics under tension state. The model is relatively simple and requires few material parameters. In addition, these parameters can be obtained from conventional experiments. The constitutive model is suitable for reinforced concrete pile subjected to monotonic loading [13].

Tab. 1. Material parameters of soil

Layer No	Thickness/m	Soil category	Shear modulus G/MPa	Poisson's ratio ν	Cohesion c/kPa	Internal friction angle φ/°	Dilatancy angle ψ/°
1	1.5	silt	30.8	0.3	2	33	3
2	5	Silty sand	57.7	0.3	0	34	4
3	4.5	Sandy silt	57.8	0.3	2	28	0
4	11	Silt sand	87.7	0.3	0	33	3
5	7	Sandy silt	87.7	0.3	2	28	0
6	-	Silty sand	87.7	0.3	0	30	0

Tab. 2. Material parameters of concrete and rebar

Material	Young's modulus E/Mpa	Poisson's ratio ν	Compressive strength f_c/MPa	Tensile strength f_{ct}/MPa
Concrete	32173	0.2	27.5	2.7
Steel	210000	0.3	-	471

In the finite element model, the mesh adopted for discretizing the soil and pile consists of 8 node reduced integration solid elements. Rebar is discretized by truss elements. To avoid the boundary effect, the diameter of the soil domain is D_s=32D, and the depth of that is L_s=41m. The lateral sides of the domain are constrained by vertical rollers, and the base is fully fixed. Mesh refinement, as shown is Figure 1, is conducted in the soil near the pile where high levels of plastic strain are expected to develop.

(a) soil domain (b) pile (c) reinforcement

Fig. 1. Finite element mesh for the soil, pile and reinforcement

The frictional contact pairs algorithm with Mohr-Coulomb criterion is used to simulate the contact response at the soil-pile interface [14]. When the normal tensile stress develops at the soil-pile interface, separation between soil and pile occurs. When the normal stress is compressive, the Coulomb friction law, as shown in Eq. (1), is used to describe the tangential friction stress,

$$\tau_{\text{crit}} = \mu p_{\text{int}} \tag{1}$$

where τ_{crit} is the critical shear stress, p_{int} is the normal stress at the interface and μ is the friction coefficient. When the tangential stress at the interface is less than τ_{crit}, the pile-soil interface keeps the bonding state, Once the tangential stress reaches the critical value, slip can occur at the soil-pile interface. In the paper, a value of $\mu = 0.6$ is selected for any soil layer.

The initial stress field within the soil domain is calculated under K_0-conditions before loading, which can eliminate the additional deformation caused by applying gravity. On the basis of the available data from Huang etc [10], it is found that the soil is submerged with buoyant unit weight γ'=9kN/m^3 and the coefficient of earth pressure at rest is K_0=0.72. After this stage, a lateral load is applied at the pile head. The magnitude of the load is progressively increased to the maximum value for which a solution is obtained successfully.

A comparison in terms of the horizontal displacement-load curve, i.e. *Q-s* curve, at the pile head is shown in Figure 2. The displacement-load curve calculated under the assumption that the pile behaves as an elastic solid is also shown in the same figure. As can be seen, the assumption of ignoring concrete damage and rebar yielding leads to a considerable underestimation of the pile deflection, however there is significantly good agreement between numerical simulation and field measurement when concrete damage and rebar yielding is considered. When the lateral load applied at the pile head is less than 480kN, the concrete stays in elastic stage, as illustrated in Figure 3(a), therefore the calculated result without considering concrete damage and rebar yielding is also consistent with the measured result. However, when the horizontal load is higher than 480kN, concrete damage begins to occur on the tension side of pile body, as indicated in gray color in Figure 3(b). With increasing the applied load, the cracking domain is expanding in the concrete, as shown in gray area of Figure 3(c) and 3(d). At the same time, the tensile stress in the steel rebar on the tension side of pile body increases gradually until the yield state is reached.

Figure 4 and 5 show the longitudinal strain-normal stress curves calculated in the elements of concrete and rebar which are affected by the highest stress level. As shown in Figure 4(b), the maximum compressive stress in the concrete is about 24.2MPa which is lower than the strength of concrete, i.e. 27.5Mpa, so failure at compression does not take place in concrete during the whole loading process. However the tensile stress of concrete and rebar does attain the respective strength which is shown in Table 2. In view of the above results, it can be concluded that a plastic hinge may form in the upper portion of the pile at the end of loading event. This failure mechanism is expected to occur in the flexible or long pile [9, 10].

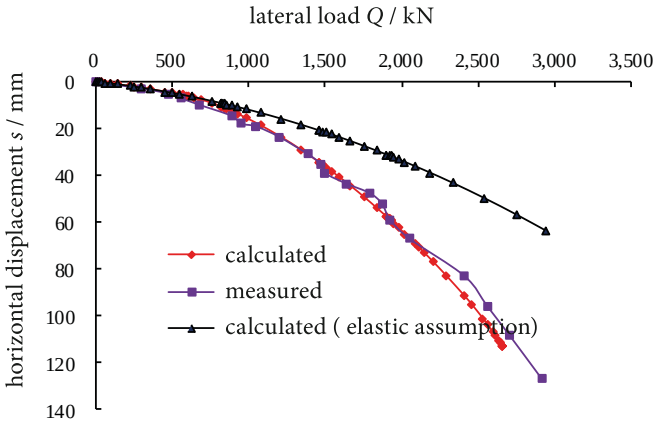

Fig. 2. Displacement curve at the pile head under lateral loading

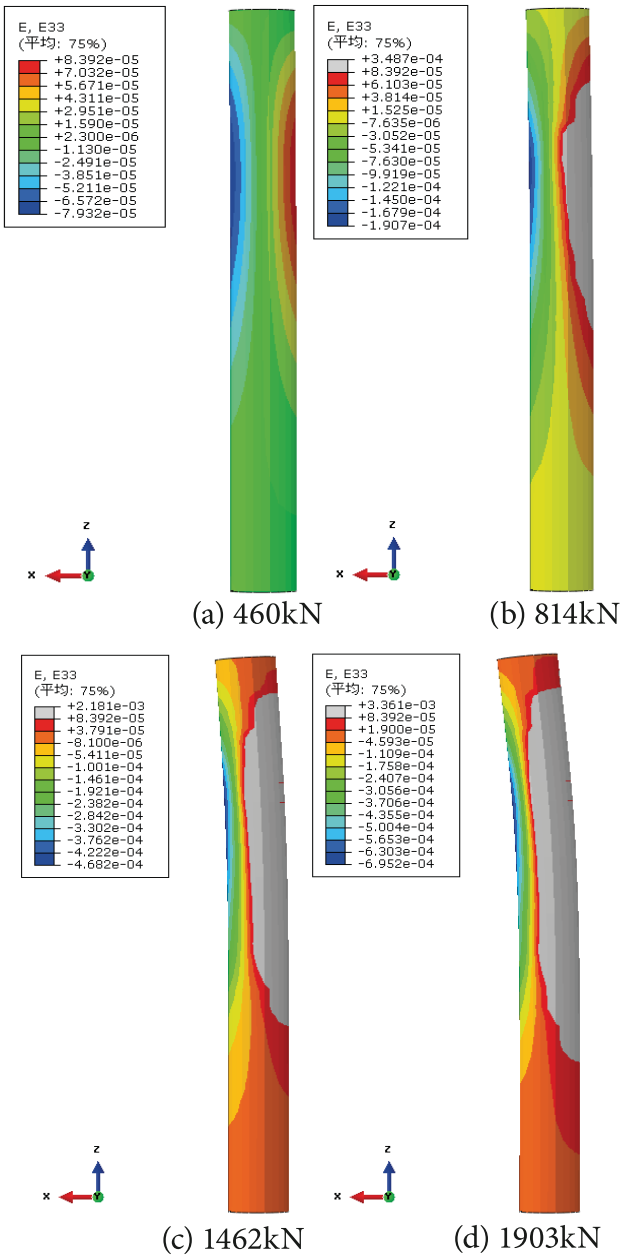

Fig. 3. Evolution of normal strain and cracking at the pile

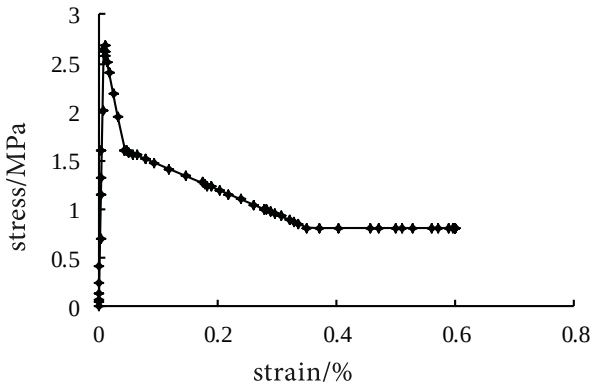

(a) tensile strain-stress relationship

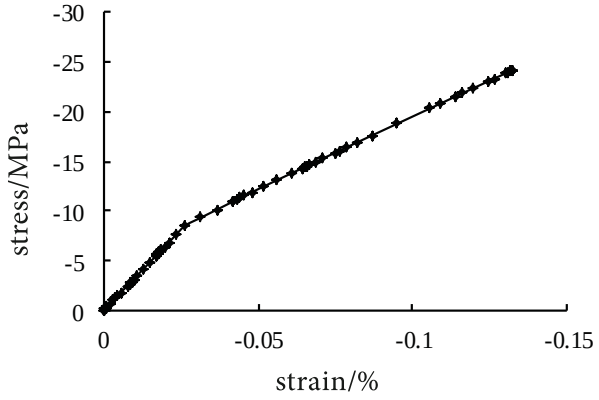

(b) compressive strain-stress relationship

Fig. 4. Curves of strain-stress relationship for concrete

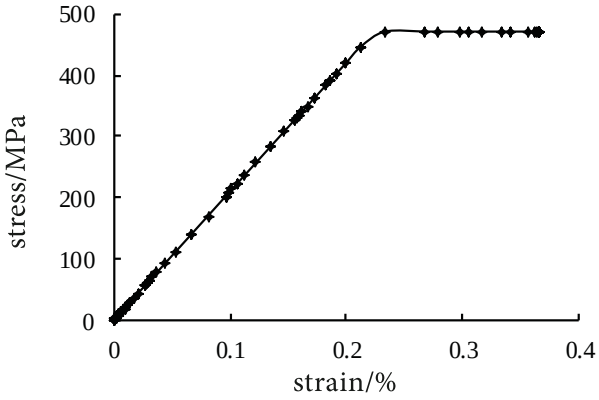

Fig. 5. Curves of strain-stress relationship for rebar

DETERMINATION METHOD OF ALLOWABLE LATERAL CAPACITY

The critical capacity and ultimate capacity are usually determined according to the strength conditions in the design of the horizontally loaded pile. Based on 'Technical code for testing of building foundations piles' of China [15], the critical capacity of single pile can be determined according to the value of lateral load corresponding to the first inflection point on the $Q-\Delta s/\Delta Q$ curve or the $Q-\sigma_s$ curve, in which σ_s is the tensile stress in the rebar located at the pile section with maximum bending moment. The ultimate capacity can be determined according to the value of lateral load corresponding to the second inflection point on the $Q-\Delta s/\Delta Q$ curve or the load that causes the steel rebar to begin to yield. For the pile with strong bending capacity, although obvious damage does not occur in the pile body, it is considered that the horizontal capacity of the pile reaches the limit state when the displacement of pile head exceeds the allowable value due to the plastic flow of soil around the pile.

According to Technical code for building pile foundations of China [15], the maximum displacement at the ground of bridge structure is not allowed to exceed 6mm. In view of the above numerical computation results, these methods are compared of selecting the allowable value of the horizontal capacity, as illustrated in Figure 2 and 6. It can be seen that the allowable capacity is $Q_{6mm}=600\text{kN}$ from Figure 2, and the value of critical load and ultimate load are respectively 690kN and 2410kN from Figure 6(b). The inflection point on the $Q-\Delta s/\Delta Q$ curve is not very significant, therefore it is suggested that determination of the critical value and limit value of single pile under lateral loading is more reliable in the light of $Q-\sigma_s$ curve. During in situ test of pile foundations in transportation infrastructure construction, the stress of the steel rebar can be monitored by embedding rebar stress gauges into the pile body, and then the $Q-\sigma_s$ curve can be obtained.

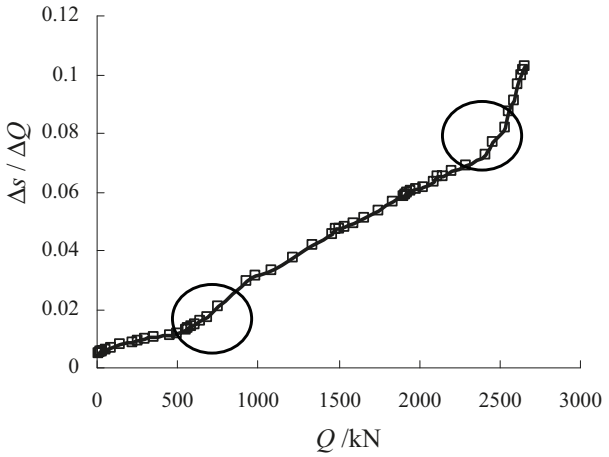

(a) $Q-\Delta s/\Delta Q$ relation

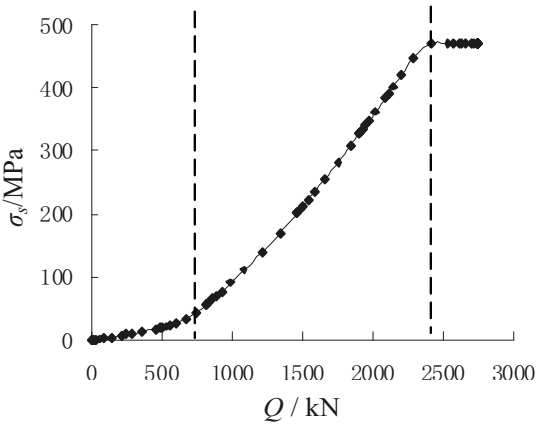

(b) $Q-\sigma_s$ relation

Fig. 6. Two curves utilized in determing lateral capacity of single pile

EFFECT OF REINFORCEMENT RATIO

With the increase of the horizontal load applied at the pile head, concrete cracks occur on the tension side of pile body, then the stress is mainly carried by the steel rebar. Therefore, it is important of reinforcement ratio to the lateral bearing capacity of pile foundations. In order to investigate influence of reinforcement ratio on the capacity of single pile, the various reinforcement ratio of the pile is shown in Table 3. In this section, the soil is uniform with the elastic modulus E = 140MPa, and internal friction angle φ = 35°.

Tab. 3. Reinforcement of piles

arrangement	Reinforcement ratio
52ϕ22	1.12%
52ϕ28	1.81%
52ϕ32	2.37%
52ϕ36	2.99%

The Q-s curve obtained at the pile head under the different reinforcement ratios is given in Figure 7. It can be seen from Figure 7 that when the horizontal load is smaller, concrete cracking does not take place on the tensile side of pile body, therefore the reinforcement ratio has little effect on the Q-s curve. However, with the increasing lateral load, the damage area of concrete is expanding gradually, and the steel rebar becomes the main tensile member, so it can be concluded that increasing the reinforcement ratio can reduce effectively the lateral deflection of pile head. In Figure 7, under the case of lateral load level Q=1500kN, when the reinforcement ratio increases from 1.12% to 2.99%, the horizontal displacement of the pile head is reduced by 40.16%.

In order to determine the allowable capacity of the pile, the curve of the rebar under the condition of different reinforcement ratio is shown in Figure 8. From Figure 8, it can be seen that the horizontal bearing capacity of the pile increases with the increase of reinforcement ratio. For the case of reinforcement ratio 1.12%, Q_{6mm}=593kN, and the critical load is 567kN, therefore the allowable value of the horizontal capacity is controlled by the cracking of the pile in such situation of low reinforcement ratio. For other cases of high reinforcement ratios, the critical load is always higher than Q_{6mm}, so the allowable value of the horizontal capacity is controlled by the horizontal displacement of pile head in such situation [16]. For example, for the case of reinforcement ratio 2.99%, Q_{6mm}=640kN, and the critical load is 760kN. When the reinforcement ratio increases from 1.81% to 2.99%, the allowable value of lateral capacity is only increased by 8%, therefore for the case of higher reinforcement ratio, the allowable value of the horizontal capacity is controlled by the displacement of pile head, and the increase of reinforcement ratio has little influence on the increase of the allowable capacity.

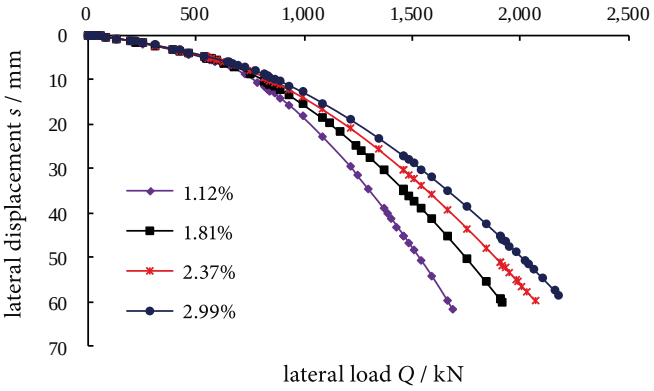

Fig. 7. Effect of reinforcement ratios on displacement of pile head

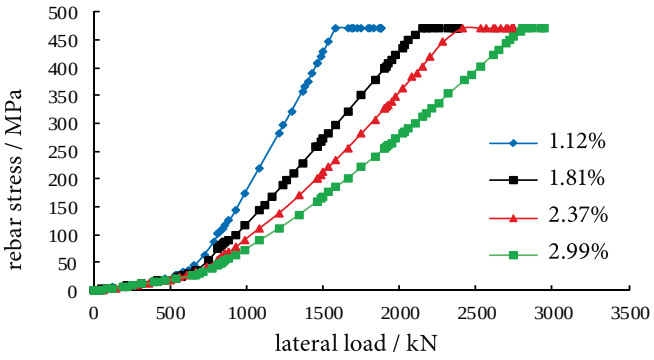

Fig. 8. Effect of reinforcement ratios on the stress of rebar

EFFECT OF VERTICAL LOAD LEVEL

In transportation engineering practice, the pile simultaneously bears the interaction of horizontal and vertical loads, and the vertical load level may have significant influence on the lateral bearing capacity of pile foundations. However, the effect of vertical load level on the lateral capacity is generally ignored during in situ loading test. In numerical computation, the vertical load is applied first at the pile head, then the vertical load is kept unchanged, before the lateral load is applied until the ultimate state is reached.

Assuming that the vertical load level is 0, 0.2, 0.4, 0.6 and 0.8 times of the vertical ultimate capacity of single pile, the horizontal displacement-load curve at the pile head is obtained. It can be seen that in the linear stage of Q-s curve, the vertical load has little effect on the lateral displacement of pile head, but with increasing vertical load level there is a significant difference between the curves with various vertical load levels. With the increase of vertical load applied at the pile head, the deflection of pile head caused by the same lateral load level is reduced, which is consistent with the conclusions of Karthigeyan et al [4, 5]. This is mainly because that the vertical load causes the compaction effect of the soil around the pile, which leads to the increase of horizontal reaction stress and friction resistance distributed

on the sides of pile [17]. Under the case of the same level of lateral load, the friction resistance on the front side of pile body increases with the increase of the vertical load. The friction resistance increases gradually from the seabed level, reaching the maximum value at the depth of 1.5*D*, then decreases until the minimum value is attained at the depth of 6*D*, and increases soon afterwards [18-20]. This scenery does also occur on the front side of the pile, except for the separation zone between pile and soil.

The profile of bending moment of pile body on the case of the lateral load *Q*=1400kN under different vertical load levels is also obtained. The bending moment of the pile increases with the increase of vertical load until the vertical load level $V = 0.6V_{ult}$ is reached [21-23]. This is mainly because that when the displacement of pile head is induced by lateral load, the vertical load leads to an additional moment in the pile body, i.e. $P-\Delta$ effect, resulting in the increase of bending moment on the tensile side of pile. Considering the existence of vertical load can alleviate the deflection of pile head, and to prevent the failure of pile under vertical load, it is concluded that the optimum vertical load level is 0.4~0.6 times of the vertical ultimate load of a single pile.

CONCLUSIONS

(1) In numerical analyses of the response of reinforced pile foundations subjected to large lateral load in transportation engineering, the influence of concrete damage and rebar yielding must be taken into account on the capacity of pile foundations.

(2) For the pile with low reinforcement ratio, the allowable lateral capacity is controlled by cracking of the concrete, however the allowable lateral capacity is determined by the displacement of pile head with high reinforcement ratio.

(3) The vertical load transferred from the superstructure can reduce the deflection of pile head subjected to lateral loading, however at the same time will increase the maximum bending moment of pile body.

ACKNOWLEDGEMENT

This work was supported by the China Postdoctoral Science Foundation (2015M581713) and Shandong Provincial Natural Science Foundation (ZR2015EM047).

REFERENCES

1. Jin, L., Junqiang, L., Xu, J.: Research of Bearing Behaviour on Bridge Piles Under Complex Geological Condition. *Beijing: China Water & Power Press*, 2015, Pp. 85-92.

2. Zheng, C., Ling, M., Guoxiong, M.: Numerical Simulation of Lateral Bearing Capacity of Flexible Micropile. *Rock and Soil Mechanics*, 2011, 32(7), Pp. 2220-2224.

3. Fan, C., Long, J.H.: Assessment of Existing Methods for Predicting Soil Response of Laterally Loaded Piles in Sand. *Computers and Geotechnics*, 2005, 32(9), Pp. 274-289.

4. Karthigeyan, S., Ramakrishna, V. V. G. S. T., Rajagopai, K.: Influence of Vertical Load on the Lateral Response of Piles in Sand. *Computers and Geotechnics*, 2008, 33(2), Pp. 121-131.

5. Karthigeyan, S., Ramakrishna, V.V.G.S.T., Rajagopai, K.: Numerical Investigation of the Effect of Vertical Load on the Lateral Response of Piles. *Journal of Geotechnical and Geoenvironmental Engineering*, 2007, 133(5), Pp. 513-521.

6. Liuyong, C., Xichang, X., Shanxiong, C.: Model Test and Numerical Simulation of Horizontal Bearing Capacity and Impact Factors for Foundation Piles in Slope. *Rock and Soil Mechanics*, 2014, 35(9), Pp. 2685-2691.

7. Gang, Z., Li, W.: Load Transfer and Bearing Capacity of Inclined Pile Under Vertical Load. *Chinese Journal of Geotechnical Engineering*, 2008, 30(12), Pp. 1796–1804.

8. Zhongxiang, C., Shannan, L., Chengyong, G.: Analysis of Lateral Response of Bored Piles Based on Concrete Damaged Plasticity Model. *Chinese Journal of Rock Mechanics and Engineering*, 2014, 33(s2), Pp. 4033-4040.

9. Conte, E., Troncone, A., Vena, M.: Nonlinear. Three-dimensional Analysis of Reinforced Concrete Piles Subjected to Horizontal Loading. *Computers and Geotechnics*, 2013, 49, Pp. 123-133.

10. Huang, A.B., Hsueh, C.K., O'Neill, M.W.: Effects of Construction on Laterally Loaded Pile Groups. *Journal of Geotechnical and Geoenvironmental Engineering*, 2001, 127(5), Pp. 385-397.

11. Qiu, G., Henke, S.: Controlled Installation of Spudcan Foundations on Loose Sand Overlying Weak Clay. *Marine Structures*, 2011, 24(4), Pp. 528-550.

12. Hillerborg, A., Modeer, M., Petersson, P.E.: Analysis of Crack Formation and Crack Growth in Concrete by Means of Fracture Mechanics and Finite Elements. *Cement and Concrete Research*, 1976, 6, Pp. 773–782.

13. Li, C., Qin, F., Yi, H.: Analysis on Static Performances of Smeared Cracking Model for Concrete in ABAQUS. *Journal of PLA University of Science and Technology*, 2007, 8(5), Pp. 478-485.

14. Maotian, L., Xiyuan, S., Xiaowei, T., Qinglai, F.: Lateral Bearing Capacity of Multi-Bucket Foundation in Soft Ground. *China Ocean Engineering*, 2010, 24(2), Pp. 333-342.

15. BCABP.: Ministry of Housing and Urban-Rural Development of the People's Republic of China, JGJ 106-2014. *Technical Code for Testing of Building Foundations Piles. Beijing: China Architecture & Building Press*, 2014.

16. Shengnan, H., Shannan, L., Zhongxiang, C.: Test Standards for Lateral Capacity of Single PHC Pile. *Chinese Journal of Geotechnical Engineering*, 2013, 35(s1), Pp. 378-382.

17. Wu, K., Fan, Q., Hao, D., Chen, R., Liu, J.: Construction Mechanics Effect of Submarine Immersed Tube Tunnel Subjected to Different Pore Pressures Based on Numerical Analysis. *Journal of the Balkan Tribological Association*, 2016, 22(3), Pp. 2447-2453.

18. Abdullah, N.A., Rashid, N.M.: Acquiring Cybercrime Evidence on Mobile Global Positioning System (Gps): Review. *Acta Electronica Malaysia*, 2017, 1(2), Pp. 17-19.

19. Basir, N.F., Kasim, S., Hassan, R., Mahdin, H., Ramli, A., Md Fudzee, M.F., Salamat, M.A.: Sweet8bakery Booking System. Acta Electronica Malaysia, 2018, 2(2), Pp. 14-19.

20. Abugalia, A., Shaglouf, M.: Analysis Of Different Models Of Moa Surge Arrester For The Transformer Protection. Acta Mechanica Malaysia, 2018, 2(2), Pp. 19-21.

21. Adrian, C., Abdullah, R., Atan, R., Jusoh, Y.Y.: Theoretical Retical Aspect In Formulating Assessment Model Of Big Data Analytics Environment. Acta Mechanica Malaysia, 2018, 2(1), Pp. 16-17.

22. Abdul Sukor, N.S., Jarani, N., Muhammad Fisal, S.F.: Analysis of Passengers' Access and Egress Characteristics to The Train Station. Engineering Heritage Journal, 2017, 1(2), Pp. 01-04.

23. Abdul Sukor, N.S., Mohd Sadullah, A.F.: Addressing the road safety results impasse through an outcome-based approach in the state of Penang, Malaysia. Engineering Heritage Journal, 2017, 1(1), Pp. 21-24.

CONTACT WITH THE AUTHORS

Fan Qinglai
e-mail: fanqinglai@foxmail.com

School of Civil Engineering
Ludong University
Yantai
China

Gao Yufeng
e-mail: yfgao@163.com

College of Civil and Transportation Engineering
Hohai University
Nanjing
China